ADVANCED FUNCTIONAL MATERIALS

DOI: 10.1002/adfm.200500468

Sequential Nucleation and Growth of Complex Nanostructured Films**

By *Thomas L. Sounart*, *Jun Liu*,* *James A. Voigt*,* *Julia W. P. Hsu*, *Erik D. Spoerke*, *Zheng (Ryan) Tian*, and *Yingbing Jiang*

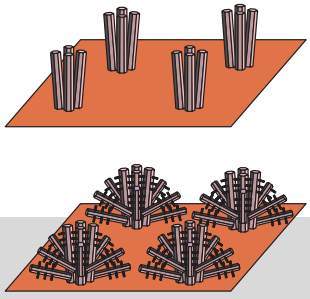

Nanostructured films with controlled architectures are desirable for many applications in optics, electronics, biology, medicine, and energy/chemical conversions. Low-temperature, aqueous chemical routes have been widely investigated for the synthesis of continuous films, and arrays of oriented nanorods and nanotubes. More recently, aqueous-phase routes have been used to produce films composed of more complex crystal structures. In this paper, we discuss recent progress in the synthesis of complex nanostructures through sequential nucleation and growth processes. We first review the use of multistage, seeded-growth methods to synthesize a wide range of nanostructures, including oriented nanowires, nanotubes, and nanoneedles, as well as laminated films, columns, and multilayer heterostructures. We then describe more recent work on the application of sequential nucleation and growth to the systematic assembly of large arrays of hierarchical, complex, oriented, and ordered crystal architectures. The multistage aqueous chemical route is shown to be applicable to several technologically important materials, and therefore may play a key role in advancing complex nanomaterials into applications.

1. Growth of Oriented Nanocrystalline Films

Nanostructured films and coatings with controlled surface area, porosity, crystalline orientation, grain sizes, and crystal morphologies are desirable for many applications, including microelectronic devices, chemical and biological sensing and diagnosis, energy conversion and storage (photovoltaic cells, batteries and capacitors, and hydrogen-storage devices), light-emitting displays, catalysis, drug delivery, separation, and optical storage. Meeting the demands of these potential applications, however, will require reliable and economic processes for the production of a large supply of high-quality nanomaterials. Gas-phase reactions[1] have been extensively used to prepare oriented nanostructures including carbon nanotubes,[2,3] ZnO nanowires,[4,5] and many other oxide and non-oxide semiconductor materials,[6,7] but these methods typically require high temperatures (~500–1100 °C) and vacuum conditions, which limit the choice of substrate and the economic viability of high-volume production. These limitations have stimulated research on solution-phase synthesis (sometimes referred to as the soft solution route or chemical bath deposition), which offers the potential for low-cost, industrial-scale manufacturing. Low-temperature (typically < 100 °C), aqueous-phase approaches are particularly attractive because of their low energy requirements, and safe and environmentally benign processing conditions.

In aqueous-phase synthesis, oriented nanocrystalline films are deposited on a substrate in aqueous media by heterogeneous nucleation and subsequent growth. The resultant film structure is controlled by a complicated set of coupled processes in both the solution and solid phases. Heterogeneous nuclea-

[*] Dr. J. Liu,[+] Dr. J. A. Voigt, Dr. T. L. Sounart, Dr. J. W. P. Hsu, Dr. E. D. Spoerke
Electronic Materials and Nanostructures Materials
Sandia National Laboratories
P.O. Box 5800, Albuquerque, NM 87185-1411 (USA)
E-mail: jun.liu@pnl.gov; javoigt@sandia.gov
Prof. Z. Tian
University of Arkansas
Fayetteville, AR 72701 (USA)
Dr. Y. B. Jiang
University of New Mexico
Albuquerque, NM 87131 (USA)
[+] Present address: Pacific Northwest National Laboratory, 902 Battelle Boulevard, Richland, WA, USA.

[**] This work is supported by the Sandia National Laboratories (SNL) Laboratory-Directed Research and Development Program (LDRD) and by the Division of Materials Sciences and Engineering, Office of Basic Energy Sciences, U.S. Department of Energy. SNL is a multiprogram laboratory operated by Sandia Corporation, a Lockheed Martin Company, for the Department of Energy under Contract DE-AC04-94AL85000. The authors thank Bonnie McKenzie and Neil Simmons (SNL) for SEM support, and Dr. Jerrold Floro (SNL) and Professor Ping Lu (New Mexico Institute of Technology) for helpful discussions on crystallography.

tion on the substrate is promoted over homogeneous precipitation in solution by controlling the precursor supersaturation levels and the interfacial energy between the substrate and the new phase to be formed.[8] Two basic approaches have been used to nucleate films: direct deposition and deposition on chemically modified interfaces using organic self-assembled monolayers (SAMs).[9] Without surface modification, the free energy of crystallization on the native substrate interface must be intrinsically low enough to relieve the supersaturation and induce direct film growth. This affects the choice of substrate and film structure for a particular solution chemistry. SAMs containing surface-active groups have been shown to promote heterogeneous nucleation by reducing the free energy of formation of the crystalline phase.[8,10,11] The functional molecules in the SAMs can be chosen to control the nucleation density and the crystalline phase and orientation. Nucleation and growth of calcium carbonate on SAMs has been extensively studied[10] because of its relevance to biomineralization,[12] and many nanostructured ceramic films, including vertically oriented iron oxide or hydroxyl oxide nanorods on SAMs, have also been reported.[13,14]

Recently, several researchers have discovered aqueous chemistries and substrates that support direct deposition of oriented nanocrystalline films. Vayssieres et al.[15,16] reported the growth of large oriented arrays of akaganeite (β-FeOOH) nanorods directly on tin oxide or alumina, with the akaganeite being converted to hematite (α-Fe_2O_3) or ferromagnetic iron nanorods via subsequent treatment. This approach was extended to ZnO by thermally decomposing metheneamine in the presence of $Zn(NO_3)_2$ to produce large arrays of oriented ZnO rods, about one to two micrometers in diameter.[17] Longer reaction times led to preferred dissolution of the ZnO rods on the metastable (0001) polar surfaces and produced hollow hexagonal microtubes.[18] Arrays of much smaller ZnO nanorods were later obtained by reducing the $Zn(NO_3)_2$ concentration.[19] The conditions for synthesizing ZnO-nanorod arrays from aqueous solutions were recently reviewed by Govender et al.,[20] and similar aqueous chemical routes have been developed to grow oriented arrays of nanorods and nanotubes of other metal chalcogenides and hydroxides.[21–25] Electrochemical deposition in aqueous solutions has also been applied to directly deposit oriented films of ZnO nanorods,[26–31] cuprous oxide nanocubes, nanopyramids,[32] and several other crystal habits.[33]

To date, most of these solution-phase synthesis methods have produced either continuous film structures or arrays of nanorods or nanotubes. Although a few studies have recently reported tower-, tube-, and flower-like morphologies resulting from the addition of organic growth modifiers,[34–36] fabrication of more complex nanostructures, such as those observed in natural materials or biominerals,[37] remains a significant challenge. In this Feature Article, we discuss multistage synthesis strategies for systematically adding complexity to oriented nanocrystals. This approach has provided an opportunity for rational design and synthesis of controlled architectures in nanostructured films.

Jun Liu recently joined the Institute for Interfacial Catalysis at the Pacific Northwest National Laboratory as a Laboratory Fellow to lead the synthesis task. He received his B.S. degree in chemical engineering from Hunan University, M.S. and Ph.D degree in materials science and engineering from University of Washington in Seattle. He has served at the Pacific Northwest National Laboratory and Lucent Bell Laboratory as a senior staff member, and as a manager at the Sandia National Laboratories. His research interests include the synthesis and understanding of self-assembled materials and complex nanocrystalline materials through controlled nucleation and growth. He is also investigating the application of these materials in chemical and biosensing, energy storage and conversion, drug delivery and catalysis. He has over one hundred publications in major technical journals, and is a frequent invited speaker at major international conferences. His work has been widely reported by many major technical and commercial journals and magazines.

James Voigt is a Principal Member of Technical Staff in the Electronic and Nanostructured Materials at Sandia National Laboratories in Albuquerque, New Mexico. After receiving his B.S. from University of Wisconsin-Eau Claire in Chemistry, he earned his Ph.D. in Chemical Engineering in 1986 from Iowa State University. Since joining Sandia in 1986, Dr. Voigt's research has focused on developing solution-phase routes to inorganic materials for electronic applications. He holds several process patents and has published numerous articles during his exploration of materials processing from the basic science of nucleation and growth in solution to process scale-up. His current areas of research include, in addition to the controlled growth of nanoscale heterostructures, the development of transparent ceramics for laser applications, the synthesis of complex ferroelectric oxides for high-energy density dielectrics, and improved-efficiency hybrid/organic inorganic solar cells.

ADVANCED FUNCTIONAL MATERIALS

2. Seeded Crystal Growth

Multistep synthesis of complex nanostructured films often begins with substrate surface preparation for heterogeneous nucleation of oriented nanocrystals. On many substrates, this can be accomplished with SAMs, but an even more straightforward approach is to seed the substrate with nanoparticles of the desired film material. We and other groups[38–55] developed seeded-growth methods that permit control over the size, population density, and spatial distribution of the crystals. Several classes of materials, such as ZnO, TiO_2, CdS, and polymers have been studied. Nanoparticles are often widely available through commercial sources or can be readily prepared using techniques reported in the literature. The seeds can be deposited on the substrate using many mature techniques, such as dip-/spin-coating,[40–42,48,52,53] sol–gel coating,[43,44] or electrophoretic deposition.[54] In most seeding techniques, the nanoparticles are produced in a separate process before physical deposition on the substrate. However, atomic layer deposition,[45] radiofrequency (RF) magnetron sputtering,[46,47,49] solution coating,[55] hydrothermal pretreatment,[50] and electrochemical deposition[38,39,51] produce a nanoparticle seed layer during an initial deposition step. Once the seed layer is formed, oriented nanocrystal growth follows in a second step. These two-step processes hint at the potential of using multiple reaction steps to control nanostructured-film synthesis.

When nanoparticles are applied as the seeds, nanocrystal orientation and alignment could be accomplished through competition.[41] Since the nuclei (or the seeds) are generally not well aligned on the substrate, the new crystal growth from these seeds will have no preferred orientation initially. However, as the crystals, such as nanorods, grow along the favored crystal planes, those that are not aligned normal to the substrate are soon impeded by neighboring crystals, and do not have room for further growth. Only the crystals with the growth orientation normal to the substrate can continue to grow, thus forming the oriented arrays. The size and population density of the seeds on the substrate primarily determines the size and population density of the oriented nanocrystals.

ZnO-nanorod arrays of highly uniform orientation were produced from epitaxial growth on <0001>-oriented seed layers.[43,55] In this case, there is no competitive growth, and the nanorod orientation is dictated by the seed orientation. Oriented seed layers have been prepared by repeatedly coating glass or silicon substrates with solutions of zinc acetate in ethanol or zinc acetate/methanolamine in methoxyethanol, followed by heat treatment at 350–800 °C. Although the fundamental mechanisms are not clear, the heat treatment produces vertically aligned nanocrystals that function as the seeds for large arrays of vertical ZnO nanowires.

The fundamental advantage of seeded growth is the enhanced control imparted by separating nanoparticle film nucleation and oriented rod growth into two steps. In each step, different experimental conditions can be used to optimize and control each one independently. Extending this concept, we have used several synthesis steps to produce oriented nanostructures that are much more complex than simple nanorod architectures (Fig. 1). In this methodology, the materials produced in one step function as the substrate for the next step. The desired nanostructures are produced by altering the experimental conditions in a controlled fashion between the different steps. For example, after seeding a glass substrate (Fig. 1a), ZnO crystals are grown along the <0001> orientations to form long prismatic nanorod arrays (Fig. 1b). In subse-

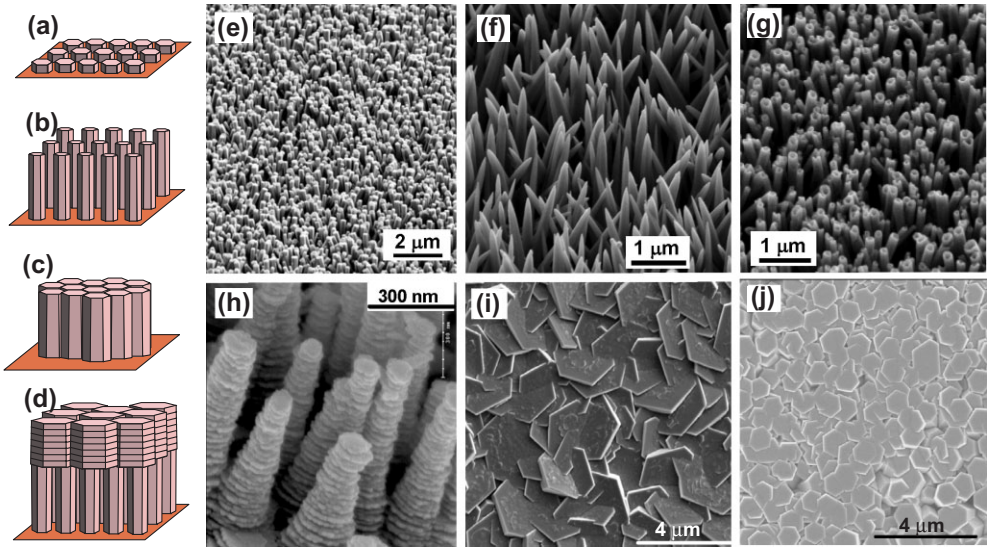

Figure 1. One-step and multistep seeded growth of large arrays of oriented nanostructured ZnO films from aqueous solution synthesis; schematic illustration (a–d) and scanning electron microscopy (SEM) images of example array structures (e–j): a) nucleation seeds on a substrate; b) oriented nanorods from seeded growth; c) densely populated ZnO-rod array from secondary growth; d) two-layer structure with one layer of nanorods and another layer of nanoplates, from multistep growth; e) nanorods; f) nanoneedles; g) nanotubes; h) stacked columns; i) nanoplates formed on nanorods; and j) dense arrays of large, oriented ZnO crystals. The structures in (e–i) were synthesized on glass microscope slides after seeding with ZnO nanoparticles; the arrays in (e–g) required one seeding step and one growth step, and those in (h–i) involved multiple growth steps after seeding.

quent steps, organic molecules are added to change the surface chemistry so that the initial rods will grow into different shapes (Figs. 1c,d). Adding citrate, for example, reduces the aspect ratio of the rods. During ZnO nanorod growth, citrate preferentially adsorbs to the (0001) surfaces, which inhibits crystal growth along the [0001] direction and produces fatter and shorter crystals.[41] By controlling various additive concentrations, and the number of growth steps, we have systematically controlled the aspect ratio of the nanorods, changed the crystal morphology from rods (Fig. 1e) to needles (Fig. 1f) to tubes (Fig. 1g) to stacked columns (Fig. 1h) and to plates (Fig. 1i), grown isolated nanorods or oriented dense films (Fig. 1j), and produced even more complicated bilayer structures.[41] Hirano et al. have also reported an aqueous multistep process to prepare oriented ZnO microcrystals similar in structure to those in Figure 1j.[56] While some of the other morphologies have also been reported using single-step synthesis, such as solution-grown micro-/nanotubes[18,47] and gas-phase-derived nanotubes and nanoneedles,[2,3,57] a key advantage afforded by the aqueous, multistage approach is the ability to systematically generate and control a diverse array of structures from an otherwise similar and inexpensive chemical route.

The multistep, seeded-growth technique is applicable to materials other than ZnO. For example, oriented conductive polymer nanowires have been produced by a multistage electropolymerization and electrochemical deposition process.[38,39] In the first step of the process, a high current density is applied to yield a dense and uniform array of polymer nanoparticles on the substrate. In subsequent steps, the current density is sequentially reduced to suppress the creation of new polymer particles and promote polymerized growth from the existing polymer seeds. Other nanocrystalline films produced via two-step, seeded growth include oriented arrays of $CaCO_3$ nanowires[51] and TiO_2-based nanotubes.[48] The oriented arrays of TiO_2-based nanotubes are grown using TiO_2-nanoparticle seeds dip-coated on Ti foil.

3. Hierarchical Crystal Growth

Two-step, seeded growth of simple one-dimensional oriented nanocrystalline films and multistage growth of more complicated nanostructures are vanguards for a process to systematically assemble complex, hierarchical crystal architectures. In the previous section, we discussed multistage aqueous reactions that have been used to tune the morphology of oriented crystalline films by altering the crystal growth behavior in each stage, but without nucleating new branched crystals after the first stage. Several groups have recently used more than one synthesis step to nucleate new oriented nanocrystals on crystals formed in a previous reaction step. In gas-phase synthesis, Dick et al.[58] first synthesized GaP and InP semiconductor nanowires, and then sequentially reseeded the nanowire surfaces to produce treelike nanostructures. In solution-phase synthesis, similar ZnO[59] and ZnO/TiO_2-based[60] composite nanostructures were produced through multistep precipitation of powders in bulk aqueous solutions. We have investigated multistep, aqueous nucleation and growth methods that have produced higher-order, hierarchical films of several important minerals. In the hierarchical growth method, the first step is to create nucleation sites, via processes such as seed deposition or micropatterning of SAMs (Fig. 2). Oriented nanocrystals grow from these nucleation sites, and in subsequent reaction steps, new crystals nucleate and grow on the crystals produced in previous stages. This provides the capability to build a diverse range of complex nanostructures from various primary subunits that can be tuned by the growth chemistry in each step.

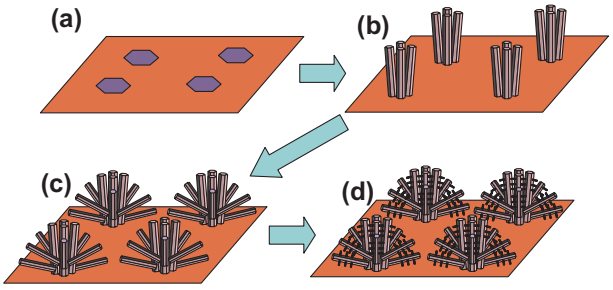

Figure 2. Schematic illustration of the multistep, sequential nucleation and growth method leading to truly hierarchical structures: a) creation of nucleation centers on a substrate by, e.g., micropatterning or microstamping; b) growth of patterned nanorods on a substrate; c) secondary growth from the patterned nanorods; and d) tertiary growth from the secondary rods.

3.1. Renucleation and Growth on ZnO

Higher-order ZnO crystal structures assembled from rod- or needle-shaped primary subunits have been synthesized with a sequential nucleation and growth process. In one approach, primary ZnO rods are first prepared on a clean glass substrate (Fig. 3a). During the second step, new crystals grow on the surfaces of the primary rods when bifunctional diaminoalkane molecules are added to the solution (Fig. 3b). The structure observed in Figure 3b is similar to the rotorlike crystals observed in homogeneously nucleated powders,[59] but further crystal growth produces extended secondary crystals of starlike or comblike morphology when viewed parallel or normal to the primary crystal *c*-axis, respectively (Fig. 3c). In the third step, the tapered secondary crystals are "healed" to the hexagonal prismatic shape, and in the fourth step, additional branch crystals nucleate from the secondary structures to form unusual wagon-wheel-like crystals (Fig. 3d). Therefore, with multiple reaction steps, new nucleation sites and a variety of large supercrystal structures can be created (Figs. 3e,f). Morphological variations between the structures, such as the size, population density, and shape of the rods in each stage, can be precisely controlled with the solution chemistry in each step.

The creation of new nucleation events that produce secondary crystal growth is a critical step for the success of the multistage approach. Without the diamine molecules, new nucleation is not observed after the primary stage, and repeated crystal growth simply increases the primary crystal size. Scanning electron microscopy (SEM), transmission electron micros-

ADVANCED FUNCTIONAL MATERIALS

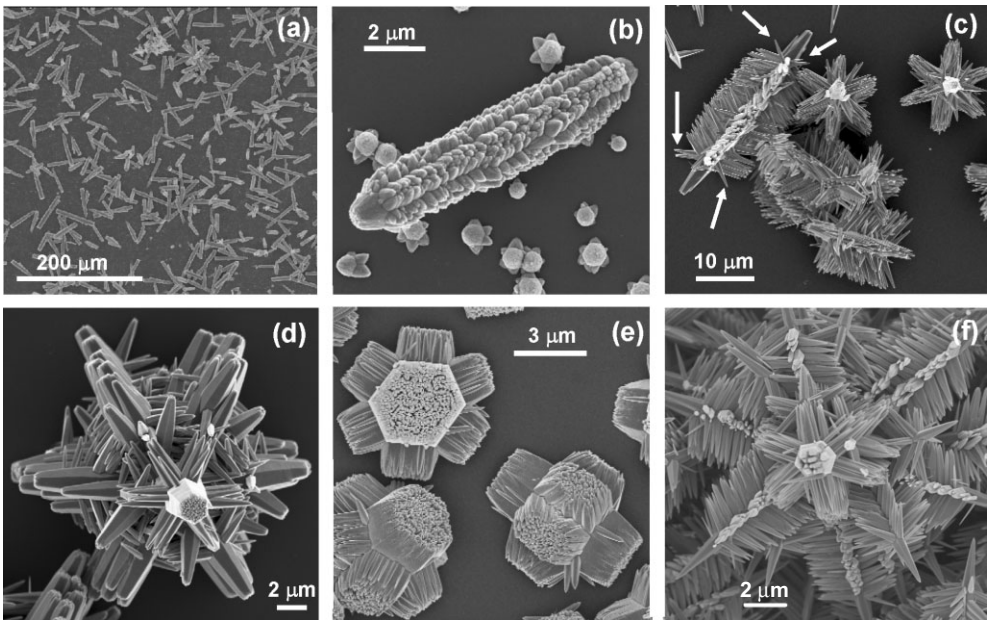

Figure 3. Hierarchical ZnO crystals formed by multistep growth (SEM images): a) primary ZnO crystals–bicrystals with the middle (0001) surface and the two flat (000$\bar{1}$) terminal surfaces; b) secondary crystals nucleated from the primary crystals; c) second-order crystal structure with long secondary crystal branches; d) tertiary crystal from renucleation on the secondary crystals in (c); e) dense arrays of secondary structures; and f) tertiary crystal with long needles from three growth stages, using diaminobutane (DAB) to nucleate branch crystals. The secondary crystal in (b) is observed at an early stage of growth (1 h), and the crystals in (c–f) have had time (at least 6 h in final growth step) to mature to equilibrium conditions.

copy (TEM), and high-resolution TEM studies have elucidated the details of the renucleation process in the presence of diaminopropane (DAP). An initial layer of polycrystalline nanoparticle seeds (bright dots in the dark-field image) nucleate without well-defined morphology or alignment (Figs. 4a–c). The dark-field TEM image (Fig. 4c), shows the polycrystalline nature of the nuclei and their misalignment with respect to the parent crystal and themselves. The possible role of diamine molecules in creating new nucleation sites on ZnO surfaces was discussed by Gao et al.,[36] who suggested that ethylene diamine (EDA) adsorbs to the high-energy sites on ZnO and reduces the surface energy, thus promoting heterogeneous nucleation. The adsorption of diamine molecules on ZnO prismatic surfaces is well documented,[35,61] and we further speculate that the diamine molecules may be bifunctional, viz., that one of the terminal amine groups binds to the existing ZnO crystal surface, and the other terminal group binds to the species in solution (Zn^{2+}, $Zn(OH)^{+}$, etc.[62]), either through electrostatic interaction or complexing.[35,61] This may induce the attachment of reactive species on the surface and cause nucleation to occur rather than epitaxially enlarge the crystals.

As the secondary branch crystals grow from the polycrystalline film, the [0001] orientation is normally tilted about $80 \pm 3°$ with respect to that of the parent crystals (Fig. 4d), and normally bends toward the center

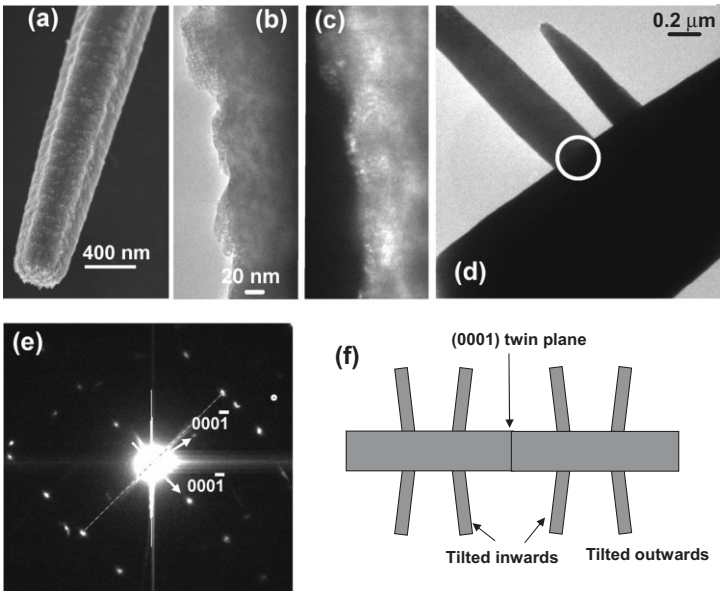

Figure 4. Secondary nucleation on primary ZnO crystals: a) polycrystalline coating of ZnO nuclei on primary ZnO crystal surface (SEM); b) bright-field TEM image of the nuclei; c) dark-field TEM image of the nuclei, showing polycrystalline nature (in dark-field TEM imaging, only diffracted light from one crystal plane is collected); d) bright-field TEM image of the interface between branched and parent crystals; e) selected-area diffraction from the interfacial region circled in (d), showing rotation and superimposition of two possibly twin-related patterns; and f) schematic illustration of (1$\bar{1}$02)-type twins showing two possible tilting angles. The primary ZnO crystals were grown on clean glass, and the secondary reaction was suspended after 30 min of incubation for (a–c) and 6 h for (d,e).

(Fig. 3c). This orientational relationship between the two crystals is also revealed in the selected-area diffraction pattern at the interface (Fig. 4e), which shows two superimposed electron diffraction patterns (wurtzite structure, $a = 3.2495$ Å and $c = 5.2069$ Å). Solution-phase syntheses of ZnO produce either bipyramidal twinned crystals that are bisected by the $(000\bar{1})$ twinning plane, or dumbbell-shaped bicrystals that are bisected by a central (0001) twinning plane.[63] In our synthesis, we exclusively observe the dumbbell-shaped twinned crystals with a flat terminal surface. The polarity is thus linkely pointed away from the terminal surface, towards the central (0001) twinning plane. The orientation of the secondary crystals that is observed experimentally in SEM images and in the superimposed diffraction pattern could be reproduced by a twining operation about a $(1\bar{1}02)$ plane. In ZnO, the calculated angle between the *c*-axes of the two crystals with this twinning relationship is 85.6°, which is in reasonably good agreement with the experimental results. However, exactly how the new crystals are related to the parent crystals as they nucleate and grow, and the nature of the interface between the crystals, are not yet well studied. It is also possible that the particular angle observed is caused by some other growth behavior, such as coincident lattice matching. Work is being done to reveal the origin of the unusual crystal growth behavior.

Figure 4f shows the two possible orientations of the secondary crystals viewed from the $(1\bar{1}02)$ zone axis, assuming that they are twin related. The branch crystals could then either tilt away from or towards the central (0001) plane. Experimentally, both configurations are observed, but the crystals tilting towards the middle plane are much more common (Fig. 3c). This difference may be caused by the lack of inversion symmetry and spontaneous dipole along the *c*-axis of ZnO crystals. The preferential selection of the tilting direction could be the result of minimizing interfacial energy during the nucleation of the secondary crystals, similar to what was suggested by Yan et al.[64] However, as indicated by the arrows in Figure 3c, sometimes (particularly near the edge of the crystals or close to a substrate surface) branch crystals are pointed outwards.

Most of the ZnO crystals observed in Figure 3 have a conical, tapered or needlelike shape owing to the presence of diamine molecules. In the literature, diamine molecules are reported to play several roles.[35,61] They can adsorb to the prismatic surfaces, either through complexing with metal ions or through electrostatic attractions, and they can also complex with metal ions in solution and thus increase mineral solubility. We have observed that cone-shaped (tapered) nanorods and nanoneedles are only produced with the addition of diaminoalkanes; growth without such diamine molecules always produces straight prismatic rods in our experiments. Secondary growth of the conical rods without the diamine actually restores the regular prismatic shape. The mechanism by which diamines direct the formation of conical rods or needles is not clear, but preferential adsorption of the diamine molecules on the prismatic surfaces may play a role; the conical surfaces are made of numerous tiny {0001} steps, and, during crystal growth, the diamine molecules may adsorb onto the prismatic surfaces and help preserve these steps.

3.2. Micropatterning of Hierarchical ZnO Films

Two-dimensional patterns of oriented nanocrystals can be created by modifying the spatial distribution of the interfacial energy on a substrate. For example, Aizenberg et al.[11,65,66] investigated the combination of SAMs and soft lithography (microstamping or microcontact printing) to prepare spatially controlled micropatterns of calcite crystals on a surface with precisely controlled location, nucleation density, size, orientation, and morphology. Mineral nucleation was favored on acid-terminated regions but suppressed in methyl-terminated regions, where the influx of nutrients was maintained below saturation. We applied similar microcontact printing techniques to grow oriented ZnO nanorods on patterned substrates.[67] Extended microarrays of carboxyl-terminated alkylthiols were printed on electron-beam-evaporated silver films. When the patterned silver substrates were placed in aqueous zinc nitrate solutions, oriented ZnO nanorods formed on the bare silver surfaces, but not on the surfaces covered by the carboxylic acid groups (Fig. 5a). Using this approach, we were able to make patterned lines, dots, and a variety of structures, and control the density and the spacing to micrometer scales (Fig. 5b). In most lines and dots, multiple nanorods were observed because the nanorods were significantly smaller than the patterns (inset in Fig. 5d). However, single crystal patterning has been obtained by growing the crystals to larger than 1 μm in size (Fig. 5b, upper inset).

We produced micropatterns of hierarchical ZnO nanorod clusters by diamine-induced sequential nucleation and growth on micropatterned primary crystals, such as those shown in Figure 5b. Secondary growth produced flowerlike crystals from new crystal growth on the top face of the primary rods and side branches formed on the edge. Figures 5c,d show arrays of ordered, flower-like ZnO structures that formed during secondary growth on a micropattern of oriented primary rods as viewed for the top and the side, and Figure 5e shows a densely packed array of similar structures in which the secondary crystals are almost connected. The variation in the orientation of the side branches arises in part from variations in the orientation of the primary rods in each bundle (Fig. 5d, inset), and in part from the effect of substrate on the relative orientation between the primary and secondary crystals. Oriented ZnO nanorods grown on silver substrates normally retain only half of the bicrystals with (0001) face at the silver interface (Fig. 5b, lower inset). The normal orientation of the secondary crystals observed for bicrystals (Figs. 3,4) would suggest that the secondary side-branch crystals should bend towards the substrate. However, the presence of the substrate physically hinders growth in that direction, and, so, many branches are tilted away from the substrate, towards the solution. Starlike or flowerlike ZnO has been observed by several groups,[35,36,61] and it has been suggested that such ZnO crystals form through $(11\bar{2}2)$ twinning, with sheets lying between spines (needles).[68] In our studies, however, $(11\bar{2}2)$ twinning is not observed.

Additional growth steps with DAP produce a pattern of tertiary structures with fine-branched crystals, such as those shown in Figure 6. Some of these small tertiary subunits also

ADVANCED FUNCTIONAL MATERIALS

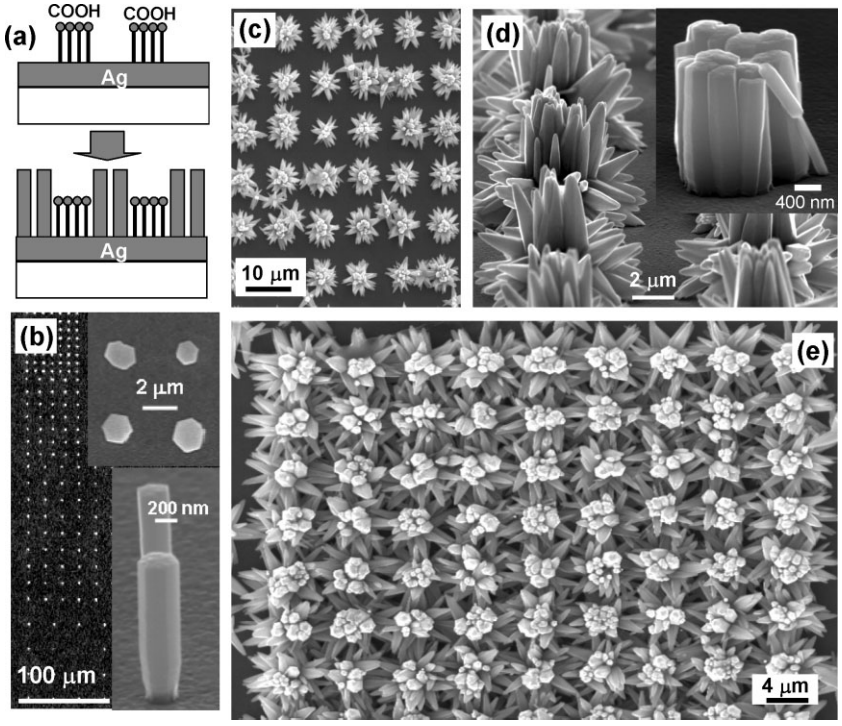

Figure 5. Micropatterning of hierarchical ZnO crystals: a) schematic illustration of micropattern chemistry for patterned ZnO growth; b) dotted patterns of vertically oriented nanorods and patterned single crystals (insets); c) micropatterned arrays of separated, secondary flowerlike structures; d) side-view of micropatterened array in (c) with the inset showing the first-generation seed bundles; e) dense micropatterned array of secondary ZnO "flowers". The patterned nanorod arrays and single crystals in (b) were synthesized on Ag substrates in one growth step after microstamping, and the flowerlike crystals in (c,d) were grown in a second stage on patterned arrays like that shown in (b, lower inset). b–e) SEM images.

nucleate sparsely on the substrate off the pattern, but it is remarkable how well the substrate is protected by only a monolayer through four reaction stages conducted over the course of several days. The length, morphology, and population density of the tertiary subunits are tunable with the reaction conditions, as discussed previously. Thus, by combining top–down micropatterning techniques with bottom–up chemical synthesis control, complex tertiary "cactus-like" crystals can be tuned in structure and organized spatially on a substrate.

3.3. Wide Applicability

The assembly of hierarchical nanocrystals by repeated nucleation and growth is not limited to the synthesis of ZnO crystals. We previously demonstrated a novel hierarchical and self-similar crystal-growth process leading to the spontaneous formation of large (of several micrometers) mesophase silicate objects in the presence of hexadecyltrimethylammoniam chloride surfactant with controlled morphology and ordering from nano- to macroscale.[69] We first created well-defined and oriented mesophase silicate crystals on a glass surface. TEM showed that these mesophase crystals have a cubic structure. The crystals are octahedral (Figs. 7a,b), truncated by the (111) surface, and oriented with one of the {111} planes parallel to the substrate. Hierarchically ordered crystals were assembled (Fig. 7a) by multistage growth; in each step, new crystals were nucleated on the existing crystals, as is the case with ZnO. Figure 7c shows the secondary structure viewed from different angles, indicating that these crystals are made of the primary octahedral subunits like those in Figure 7b. The secondary structure is about 11 μm in width — two times the size of the primary structure — and is based on a quartet–octahedron model with 24 edge-sharing octahedral primary subunits. The model contains four surfaces made of six subunits and six corners made of four subunits. Figure 7d shows tertiary structures, and the inset shows how the new crystals nucleated on the edge of the existing crystals; higher-order structures can be derived by continued edge-sharing growth (Fig. 7e). These large mesophase crystals are remarkable in several ways. First, these structures are not close-packed and contain large empty spaces, but they still have almost perfect octahedral shapes. Second, the octahedral subunits in the large structure are all about 5 μm in size and are fairly uniform. These subunits are also well aligned throughout the crystal by edge sharing. Finally, the high-order octahedral mesophase crystals are also uniform in size.

One of the important extensions of stepwise materials assembly is its application to mixed material systems. We have recently demonstrated stepwise assembly of hierarchical heterostructures by growing cadmium sulfide (CdS) nanorods on ZnO crystals (Figs. 7f,g). This process involves first nucleating and growing ZnO hexagonal rods, as described above. In a second step, CdS nanoseeds are nucleated on the ZnO crystal surfaces from a solution containing cadmium nitrate and thioacetamide as a sulfur source. This process relies on the gradual release of free sulfide ions from thioacetamide during gentle heating, which prevents massive homogeneous nucleation of CdS, and allows for heterogeneous nucleation of CdS on ZnO rods (Fig. 7f). In the third growth step, this CdS layer serves both to protect the ZnO and to seed the growth of CdS rods in a harsh reaction solution containing cadmium nitrate, thiourea, and EDA at elevated temperature and pressure. This multistep process effectively produces nanorods of CdS radiating outwards from ZnO-rod substructures (Fig. 7g). Though the mechanisms for CdS-rod formation have not yet been elucidated, the evolution of this rod morphology is attributed to the influence of EDA, much like the secondary rod growth described for ZnO is tied to the presence of diamines. This example of mixed material assembly demonstrates the wider applicability of the multistage growth process and reiterates the importance of organic growth modifiers, such as diamines, in controlling selective stages of assembly.

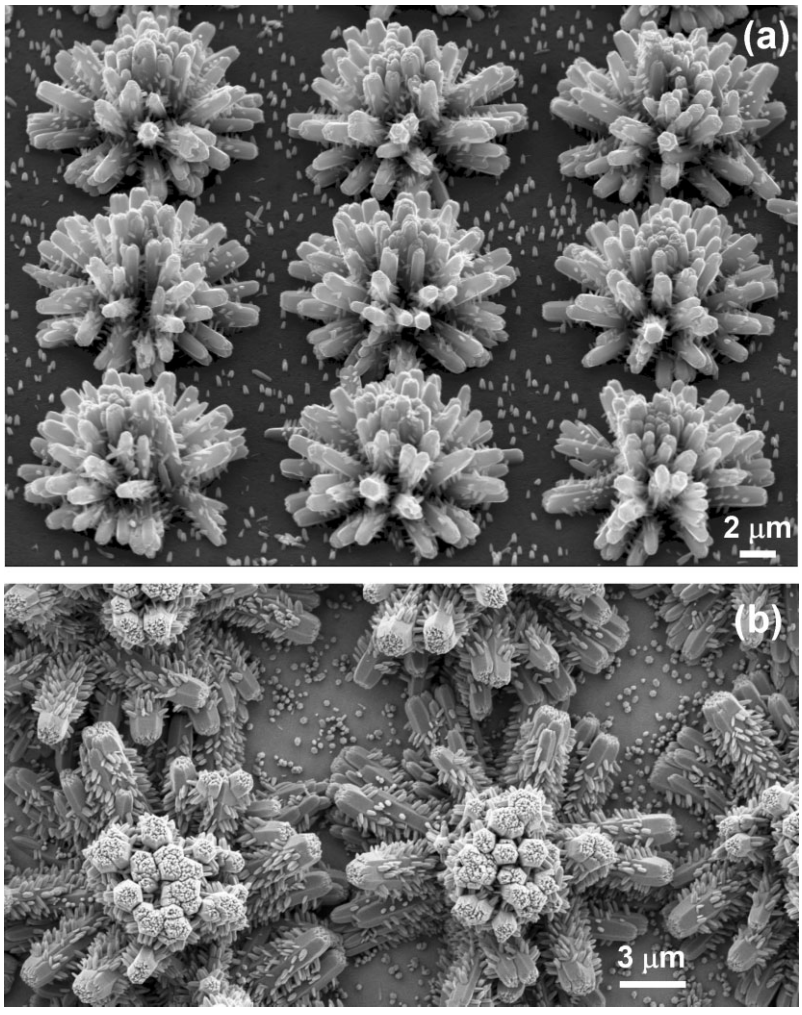

Figure 6. Micropatterned array of tertiary ZnO "cactus" structures (SEM images), produced with four growth stages on a microstamped Ag substrate: a) micropatterned array viewed at an oblique angle and b) dense array viewed normal to the substrate.

4. Concluding Remarks

While important discoveries continue to be made in nanomaterials research, the field is advancing towards the development of applications. Oriented nanocrystalline semiconductor films are receiving increasing attention because of their powerful optical and electronic properties. High-quality crystallinity, orientational alignment, and high surface/volume ratios are all important for efficient electron and photon transport in applications such as photovoltaics[49,70] and lasers.[71] With ZnO, large nanorod arrays of exceptional uniformity, orientational alignment, and optical properties (negligible defect emission) have been produced by the aqueous solution route.[43,46,47,49,52,55,72,73] Room-temperature UV lasing has also been demonstrated,[52,74] and water-repellent superhydrophobic surfaces with contact angles greater than 160° have been synthesized from ZnO nanorod arrays grown in aqueous solution.[75–77]

Most of the progress towards applications has been with ZnO because of the established morphological control and because it is a multifunctional material of great engineering significance. However, as discussed in the current article, research on materials such $CaCO_3$ and SiO_2 inspired many of the developments that have led to the progress with ZnO, which may in turn inspire further progress with other materials. Research on other nanostructured film materials, such as TiO_2, Cu_2O, and CdS, is in a nascent stage, and synthesis of complex nanostructures has just begun.

This progress notwithstanding, the potential for nanostructured films still remains largely untapped. Fulfilling this potential will require greater control of film properties, informed by a better understanding of nanocrystal nucleation and growth phenomena. Developments in solution-phase synthesis have been mostly empirically derived, and mechanisms offered in the literature have been qualitative, speculative, and incomplete. Extensive and systematic studies are needed to elucidate the principles governing the control of the observed crystalline morphologies. The fundamental mechanisms controlling renucleation and growth on existing crystals are also not well understood, and it is not clear how single crystal formation and epitaxial alignment is achieved from polycrystalline renucleation layers. Furthermore, the factors that control the surface chemistry and the crystal morphologies and sizes cannot be systematically predicted. These scientific questions will need to be addressed in future studies in order to gain the control and reliability required by nanomaterials applications. With this improved understanding and concomitant control, stepwise solution-phase growth methods should provide versatile and powerful industrial-scale production processes for assembling complex nanostructured films by design, and may ultimately be instrumental in moving nanoscience out of the laboratory and into technology.

5. Experimental

Large oriented arrays of nanoneedles were synthesized on glass substrates by seeding the slide with ZnO nanoparticles [41], followed by growth in an aqueous $Zn(NO_3)_2$ solution at 60 °C. Seeded substrates were incubated overnight at 60 °C in 125 mL Teflon bottles filled with 75 mL of an aqueous solution of 20 mM $Zn(NO_3)_2$ and hexamethyltetramine (HMT), and 130 mM DAP. The seeded side of the substrate was uniformly coated with a continuous white film comprised of an oriented array of ~100 nm wide needle-shaped crystals with approximately 10 nm tip radii.

Hierarchical ZnO crystals were synthesized on clean, unseeded glass substrates to produce a sparsely populated film of crystalline structures. Primary rods formed during incubation at 60 °C overnight in an aque-

ADVANCED FUNCTIONAL MATERIALS

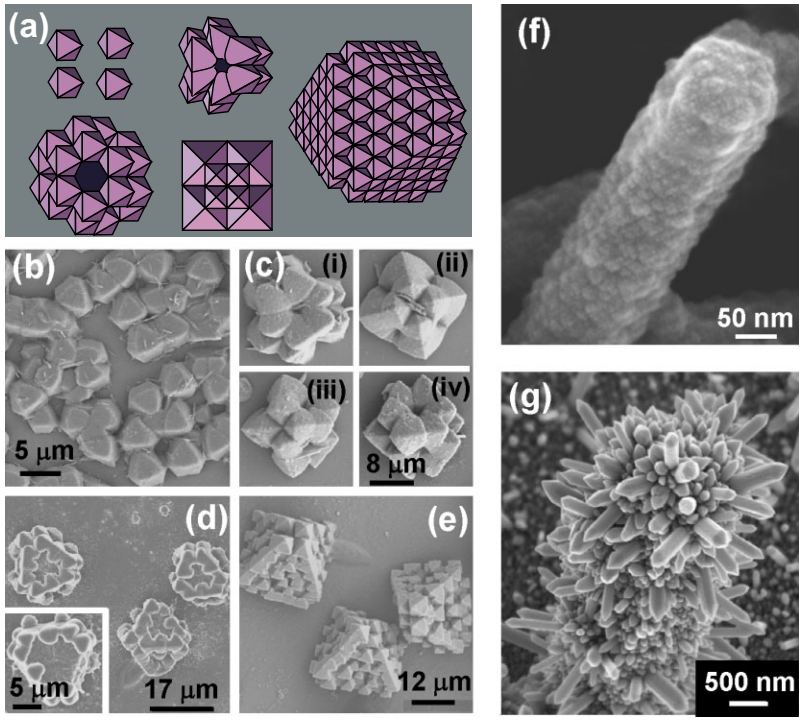

Figure 7. Higher-order structures beyond ZnO: a) schematic illustration of assembling higher-order structures by nucleating new crystals through edge-sharing configuration; b) octahedral primary crystals formed from the cubic self-assembled silicate; c) secondary structures formed from 24 primary crystals and viewed from different angles; d) tertiary structures; the nuclei on the secondary structure are visible in the inset; e) higher-order structures; f) ZnO nanorod coated with CdS nanoparticle seeds; g) CdS nanorods on ZnO crystal. CdS nanorods in (g) were grown on ZnO rods after pretreatment with CdS seeds as in (f), requiring three growth stages. (b–g) are SEM images. (a–e) are reproduced from [69].

ous solution of 20 mM $Zn(NO_3)_2$ and HMT. After drying in air, the substrates were incubated again at 60 °C for 6 h in a solution of 20 mM $Zn(NO_3)_2$ and HMT, and a DAP concentration ranging from 0.08 mM to 0.13 mM or a diaminobutane concentration ranging from 0.4 to 0.7 M, which produced oriented secondary nanocrystal arrays with tunable morphology. In order to renucleate ZnO on the needle-shaped, secondary crystals, a "healing" growth stage without diamines was usually required (three days incubation in 20 mM $Zn(NO_3)_2$ and HMT). This converted the secondary needles to hexagonal prismatic rods, and incubation in a fourth stage with diamine produced oriented arrays of tertiary nanoneedles on the secondary rods.

Ag-coated substrates were microstamped with two-dimensional patterns of carboxyl- and methyl-terminated SAMs, and then incubated at 60 °C in an aqueous solution of 20 mM $Zn(NO_3)_2$ and HMT [67]. A second stage of incubation in an aqueous solution of 20 mM $Zn(NO_3)_2$ and HMT, and 80 mM DAP produced arrays of secondary flower-like crystals, and after a healing stage in 20 mM $Zn(NO_3)_2$ and HMT, oriented tertiary nanoneedles grew on the secondary rods in a fourth stage with 40 mM DAP. The length and width of the branch crystals were controlled by the DAP concentration. A higher concentration of DAP was used in the second stage compared to in the final stage to produce crystals with smaller tertiary nanoneedles on larger secondary branches.

Films of primary ZnO rods were grown on clean or seeded glass substrates by incubation overnight at 60 °C in an aqueous solution of 20 mM $Zn(NO_3)$ and HMT [41]. After drying in air, the substrates were incubated again at 60 °C in an aqueous solution of 10 mM $Cd(NO_3)_2$ and 10 mM thioacetamide for 60 min, which nucleated a continuous seed layer of CdS nanoparticles on the primary ZnO rods. In a third growth stage, the substrates were incubated at 180 °C for 2 days in a 20 % (w/w) aqueous EDA solution, with 50 mM $Cd(NO_3)_2$ and 75 mM thiourea, which produces a continuous coating of CdS nanorods projecting from the primary ZnO rods.

Received: July 14, 2005
Final version: August 26, 2005

[1] R. Wagner, W. Ellis, *Appl. Phys. Lett.* **1964**, *4*, 89.
[2] W. Z. Li, S. S. Xie, L. X. Qian, B. H. Chang, B. S. Zou, W. Y. Zhou, R. A. Zhao, G. Wang, *Science* **1996**, *274*, 1701.
[3] Z. F. Ren, Z. P. Huang, J. W. Xu, J. H. Wang, P. Bush, M. P. Siegel, P. N. Provencio, *Science* **1998**, *282*, 1105.
[4] M. Huang, S. Mao, H. Feick, H. Yan, Y. Wu, H. Kind, E. Weber, R. Russo, P. Yang, *Science* **2001**, *292*, 1897.
[5] M. H. Huang, Y. Wu, H. Feick, N. Tran, E. Weber, P. Yang, *Adv. Mater.* **2001**, *13*, 113.
[6] D. P. Yu, Y. J. Xing, Q. L. Hang, H. F. Yang, J. Xu, Z. H. Xi, S. Q. Feng, *Physica E* **2001**, *9*, 305.
[7] L. C. Chen, S. W. Chang, C. S. Chang, C. Y. Wen, J.-J. Wu, Y. F. Chen, Y. S. Huang, K. H. Chen, *J. Phys. Chem. Solids* **2001**, *62*, 1567.
[8] B. C. Bunker, P. C. Rieke, B. J. Tarasevich, A. A. Campbell, G. E. Fryxell, G. L. Graff, L. Song, J. Liu, J. W. Virden, *Science* **1994**, *264*, 48.
[9] T. Niesen, M. De Guire, *J. Electroceram.* **2001**, *6*, 169.
[10] L. Addadi, J. Moradian, E. Shay, N. G. Maroudas, S. Weiner, *Proc. Natl. Acad. Sci. USA* **1987**, *84*, 2732.
[11] J. Aizenberg, A. Black, G. Whitesides, *Nature* **1999**, *398*, 495.
[12] S. Weiner, *Crit. Rev. Biochem.* **1986**, *20*, 365.
[13] P. C. Rieke, B. D. Marsh, L. L. Wood, B. J. Tarasevich, J. Liu, L. Song, G. E. Fryxell, *Langmuir* **1995**, *11*, 318.

[14] B. J. Tarasevich, P. C. Rieke, J. Liu, *Chem. Mater.* **1996**, *8*, 292.
[15] L. Vayssieres, N. Beermann, S. E. Lindguist, A. Hagfeldt, *Chem. Mater.* **2001**, *13*, 233.
[16] L. Vayssieres, L. Rabenberg, A. Manthiram, *Nano Lett.* **2002**, *2*, 1393.
[17] L. Vayssieres, K. Keis, S.-E. Linquist, A. Hagfeldt, *J. Phys. Chem. B* **2001**, *105*, 3350.
[18] L. Vayssieres, K. Keis, A. Hagfeldt, S.-E. Linquist, *Chem. Mater.* **2001**, *13*, 4395.
[19] L. Vayssieres, *Adv. Mater.* **2003**, *15*, 464.
[20] K. Govender, D. S. Boyle, P. B. Kenway, P. O'Brien, *J. Mater. Chem.* **2004**, *14*, 2575.
[21] W. Zhang, X. Wen, S. Yang, *Inorg. Chem.* **2003**, *42*, 5005.
[22] W. Zhang, X. Wen, S. Yang, Y. Berta, Z. L. Wang, *Adv. Mater.* **2003**, *15*, 822.
[23] L. Zhang, J. C. Yu, M. Mo, L. Wu, Q. Li, K. W. Kwong, *J. Am. Chem. Soc.* **2004**, *126*, 8116.
[24] H. Hou, Y. Xie, Q. Li, *Cryst. Growth Des.* **2005**, *5*, 201.
[25] Y. Li, Z. Wang, X.-D. Ma, X.-F. Qian, J. Yin, Z.-K. Zhu, *J. Solid State Chem.* **2004**, *177*, 4386.
[26] S. Peulon, D. Lincot, *J. Electrochem. Soc.* **1998**, *145*, 864.
[27] R. Konenkamp, K. Boedecker, M. C. Lux-Steiner, M. Poschenrieder, E. Zenia, C. Leavy-Clement, *Appl. Phys. Lett.* **2000**, *77*, 2575.
[28] M. Wong, A. Berenov, X. Qi, M. Kappers, Z. Barber, B. Illy, Z. Lockman, M. Ryan, J. MacManus-Driscoll, *Nanotechnology* **2003**, *14*, 968.
[29] M. Izaki, T. Omi, *Appl. Phys. Lett.* **1996**, *68*, 2439.
[30] B. Canava, D. Lincot, *J. Appl. Electrochem.* **2000**, *30*, 711.
[31] R. Liu, A. A. Vertegel, E. W. Bohannan, T. A. Sorenson, J. A. Switzer, *Chem. Mater.* **2001**, *13*, 508.
[32] R. Liu, F. Oba, E. W. Bohannan, F. Ernst, J. A. Switzer, *Chem. Mater.* **2003**, *15*, 4882.
[33] M. J. Siegfried, K.-S. Choi, *Adv. Mater.* **2004**, *16*, 1743.
[34] M. Maosong, J. C. Yu, L. Zhang, S.-K. A. Li, *Adv. Mater.* **2005**, *17*, 756.
[35] Z. Wang, X.-F. Qian, J. Yin, Z.-K. Zhu, *Langmuir* **2004**, *20*, 3441.
[36] X. Gao, X. Li, W. Yu, *J. Phys. Chem. B* **2005**, *109*, 1155.
[37] A. Jackson, J. Vincent, R. Turner, *Proc. R. Soc. London Ser. B* **1988**, *234*, 415.
[38] L. Liang, J. Liu, J. C. F. Windisch, G. J. Exarhos, Y. Lin, *Angew. Chem. Int. Ed.* **2002**, *41*, 3665.
[39] J. Liu, Y. Lin, L. Liang, J. A. Voigt, D. L. Huber, Z. R. Tian, E. Coker, B. Mckenzie, M. J. Mcdermott, *Chem. Eur. J.* **2003**, *9*, 604.
[40] Z. Tian, J. A. Voigt, B. M. J. Liu, M. J. Mcdermott, *J. Am. Chem. Soc.* **2002**, *124*, 12 954.
[41] Z. R. Tian, J. A. Voigt, J. Liu, B. Mckenzie, M. J. Mcdermott, R. T. Cygan, L. J. Criscenti, *Nat. Mater.* **2003**, *2*, 821.
[42] L. E. Greene, M. Law, J. Goldberger, F. Kim, J. C. Johnson, Y. Zhang, R. J. Saykally, P. Yang, *Angew. Chem. Int. Ed.* **2003**, *42*, 3031.
[43] S. Yamabi, H. Imai, *J. Mater. Chem.* **2002**, *12*, 3773.
[44] C.-H. Hung, W.-T. Whang, *Mater. Chem. Phys.* **2003**, *82*, 705.
[45] Q. C. Li, V. Kumar, Y. Li, H. T. Zhang, T. J. Marks, R. P. H. Chang, *Chem. Mater.* **2005**, *17*, 1001.
[46] S.-C. Liou, C.-S. Hsiao, S.-Y. Chen, *J. Cryst. Growth* **2005**, *274*, 438.
[47] H. Yu, Z. Zhang, M. Han, X. Hao, F. Zhu, *J. Am. Chem. Soc.* **2005**, *127*, 2378.
[48] Z. Tian, J. Voigt, J. Liu, B. McKenzie, H. Xu, *J. Am. Chem. Soc.* **2003**, *125*, 12 384.
[49] R. B. Peterson, C. L. Fields, B. A. Gregg, *Langmuir* **2004**, *20*, 5114.
[50] D. S. Boyle, K. Govender, P. O'Brien, *Chem. Commun.* **2002**, 80.
[51] D. Zhou, E. Anoishkina, V. Desai, K. Casey, *Electrochem. Solid-State Lett.* **1998**, *1*, 133.
[52] J. Choy, E. Jang, J. Won, J. Chung, D. Jang, Y. Kim, *Adv. Mater.* **2003**, *15*, 1911.
[53] J.-H. Choy, E.-S. Jang, J.-H. Won, J.-H. Chung, D.-J. Jang, Y.-W. Kim, *Appl. Phys. Lett.* **2004**, *84*, 287.
[54] E. Wong, P. Searson, *Appl. Phys. Lett.* **1999**, *74*, 2939.
[55] L. E. Greene, M. Law, D. H. Tan, M. Montano, J. Goldberger, G. Somorjai, P. Yang, *Nano Lett.* **2005**, *5*, 1231.
[56] S. Hirano, K. Masuya, M. Kuwabara, *J. Phys. Chem. B* **2004**, *108*, 4576.
[57] W. I. Park, G.-C. Yi, M. Kim, S. J. Pennycook, *Adv. Mater.* **2002**, *14*, 1841.
[58] K. A. Dick, K. Deppert, M. Larsson, T. Martensson, W. Seifert, L. Wallenberg, L. Samuelson, *Nat. Mater.* **2004**, *3*, 380.
[59] X. Gao, Z. Zheng, H. Zhu, G. Pan, J. Bao, F. Wu, D. Song, *Chem. Commun.* **2004**, 1428.
[60] H. Yang, H. Zeng, *J. Am. Chem. Soc.* **2005**, *127*, 270.
[61] B. Liu, H. Zeng, *Langmuir* **2004**, *20*, 4196.
[62] J. C. F. Baes, R. E. Mesmer, *The Hydrolysis of Cations*, John Wiley & Sons, New York **1976**.
[63] B. G. Wang, E. W. Shi, W. Z. Zhong, *Cryst. Res. Technol.* **1998**, *33*, 937.
[64] Y. Yan, M. M. Al-Jassim, M. Chisholm, L. Boatner, S. Pennycook, M. Oxley, *Phys. Rev. B* **2005**, *71*, 041 309.
[65] J. Aizenberg, *J. Cryst. Growth* **2000**, *211*, 143.
[66] J. Aizenberg, *Adv. Mater.* **2004**, *16*, 1295.
[67] J. Hsu, Z. Tian, N. Simmons, C. Matzke, J. Voigt, J. Liu, *Nano Lett.* **2005**, *5*, 83.
[68] R. McBride, J. Kelly, D. McCormack, *J. Mater. Chem.* **2003**, *13*, 1196.
[69] Z. R. Tian, J. Liu, J. A. Voigt, B. Mckenzie, X. Huifang, *Angew. Chem. Int. Ed.* **2003**, *42*, 413.
[70] M. Law, L. E. Greene, J. C. Johnson, R. Saykally, P. Yang, *Nat. Mater.* **2005**, *4*, 455.
[71] P. Yang, H. Yan, S. Mao, R. Russo, J. Johnson, R. Saykally, N. Morris, J. Pham, R. He, H. Choi, *Adv. Funct. Mater.* **2002**, *12*, 323.
[72] Q. Tang, W. Zhou, J. Shen, W. Zhang, L. Kong, Y. Qian, *Chem. Commun.* **2004**, 712.
[73] Y. W. Koh, M. Lin, C. K. Tan, Y. L. Foo, K. P. Loh, *J. Phys. Chem. B* **2004**, *108*, 11 419.
[74] K. Govender, D. S. Boyle, P. O'Brien, D. Binks, D. West, D. Coleman, *Adv. Mater.* **2002**, *14*, 1221.
[75] X. Feng, L. Feng, M. Jin, J. Zhai, L. Jiang, D. Zhu, *J. Am. Chem. Soc.* **2004**, *126*, 62.
[76] X.-T. Zhang, O. Sato, A. Fujishima, *Langmuir* **2004**, *20*, 6065.
[77] X. Wu, L. Zheng, D. Wu, *Langmuir* **2005**, *21*, 2665.